

1-21-2015

# Uptake and accumulation of bulk and nanosized cerium oxide particles and ionic cerium by radish (*Raphanus sativus* L.).

Weilan Zhang

*Southern Illinois University Carbondale*

Stephen D. Ebbs

*Southern Illinois University Carbondale, sebbs@plant.siu.edu*

Craig Musante

*The Connecticut Agricultural Experiment Station*

Jason C. White

*The Connecticut Agricultural Experiment Station*

Cunmei Gao

*Shanghai Ocean University*

~~Follow this and additional~~ works at: [http://opensiuc.lib.siu.edu/pb\\_pubs](http://opensiuc.lib.siu.edu/pb_pubs)

This document is the Accepted Manuscript version of a Published Work that appeared in final form in the *Journal of agricultural and food chemistry*, copyright © American Chemical Society after peer review and technical editing by the publisher. To access the final edited and published work see <http://dx.doi.org/10.1021/jf5052442>.

## Recommended Citation

Zhang, Weilan, Ebbs, Stephen D., Musante, Craig, White, Jason C., Gao, Cunmei and Ma, Xingmao. "Uptake and accumulation of bulk and nanosized cerium oxide particles and ionic cerium by radish (*Raphanus sativus* L.)." *Journal of agricultural and food chemistry* 63, No. 2 (Jan 2015). doi:10.1021/jf5052442.

---

**Authors**

Weilan Zhang, Stephen D. Ebbs, Craig Musante, Jason C. White, Cunmei Gao, and Xingmao Ma

**Uptake and Accumulation of Bulk and Nano-sized Cerium Oxide Particles and  
Ionic Cerium by Radish (*Raphanus sativus L.*)**

Weilan Zhang<sup>1</sup>, Stephen D. Ebbs<sup>2</sup>, Craig Musante<sup>3</sup>, Jason C. White<sup>3</sup>, Cunmei Gao<sup>1,4</sup>,  
Xingmao Ma<sup>1,\*</sup>

<sup>1</sup>Department of Civil and Environmental Engineering, Southern Illinois University;  
Carbondale, IL, 62901

<sup>2</sup>Department of Plant Biology and Center for Ecology, Southern Illinois University,  
Carbondale, IL, 62901

<sup>3</sup>Department of Analytical Chemistry, The Connecticut Agricultural Experiment Station,  
123 Huntington Street, New Haven, CT 06504, USA

<sup>4</sup>College of Marine Sciences, Shanghai Ocean University, Shanghai, 201306, China

\*Corresponding author

Xingmao Ma

Department of Civil and Environmental Engineering

Southern Illinois University Carbondale

Carbondale, IL, USA, 62901

Ph: 618-453-7774

Fax: 618-453-3044

Email: [ma@engr.siu.edu](mailto:ma@engr.siu.edu)

## **Abstract**

The potential toxicity and accumulation of engineered nanomaterials (ENMs) in agricultural crops has become an area of great concern and intense investigation. Interestingly, while below ground vegetables are most likely to accumulate the highest concentrations of ENMs, little work has been done investigating the potential uptake and accumulation of ENMs for this plant group. The overall objective of this study was to evaluate how different forms of cerium (bulk cerium oxide, cerium oxide nanoparticles, and the cerium ion) affected the growth of radish (*Raphanus sativus L.*) and accumulation of cerium in the radish tissues. Ionic cerium ( $\text{Ce}^{3+}$ ) had a negative effect on radish growth at 10 mg  $\text{CeCl}_3$  /L while bulk cerium oxide ( $\text{CeO}_2$ ) enhanced plant biomass at the same concentration. Treatment with 10 mg/L cerium oxide nanoparticles ( $\text{CeO}_2$  NPs) had no significant effect on radish growth. Exposure to all forms of cerium resulted in the accumulation of this element in radish tissues, including the edible storage root. However, the accumulation patterns and their effect on plant growth and physiological processes varied with the characteristics of cerium. This study provides a critical frame of reference on the effects of  $\text{CeO}_2$  NPs vs. their bulk and ionic counterparts on radish growth.

## **Keywords**

Cerium oxide, Nanomaterials, Nanoparticles, Radish, Phytotoxicity, Plant uptake

1 **Introduction**

2

3 Nanotechnology is a rapidly expanding global industry. Engineered nanomaterials  
4 (ENMs) with their size smaller than 100 nm in at least two dimensions are increasingly  
5 found in commercial products. Due to their small size and large specific surface area,  
6 ENMs exhibit novel and different physical, chemical and biological properties from their  
7 bulk or ionic counterparts. These unique properties provide new opportunities to fight  
8 diseases, enhance energy efficiency and improve the environment (1,2,3).

9 While the synthesis of ENMs adds desirable physical and/or chemical properties  
10 over the bulk or ionic forms, the potential environmental health and safety implications of  
11 ENM uses have become a serious concern. Previous research has shown that some ENMs  
12 used in consumer products are released into the environment and many of these materials  
13 are detected in wastewater streams (4,5,6). As one of the most commonly employed  
14 nanomaterials, cerium oxide nanoparticles (CeO<sub>2</sub> NPs) have attracted great attention. The  
15 potential toxicity of CeO<sub>2</sub> NPs (6-40 nm, unmodified) to bacteria, fish, and mammalian  
16 cells has been reported (7,8). Plants play a critical role in maintaining ecosystem health  
17 and function and as a food source for humans. Plant uptake of ENMs represents an  
18 important pathway for human exposure to these nanoparticles through food consumption  
19 (9). Consequently, investigation of the uptake and accumulation of ENMs by agricultural  
20 crops is not only warranted but also critical to food safety and human health. However,  
21 there are only a small number of studies in the literature that have addressed the  
22 interactions of CeO<sub>2</sub> NPs with terrestrial plants (10-16). In one study, Wang et al. (10)  
23 found that uncoated CeO<sub>2</sub> NPs (< 25nm) at 0.1-10 mg/L had a slightly positive effect on  
24 tomato (*Solanum lycopersicum* L.) growth and yield (e.g. increased production of tomato

25 fruit at 10 mg/L). However, cerium was reportedly transported from roots to shoots and  
26 accumulated in edible tissues, although the chemical form of Ce was not determined.  
27 These authors further investigated the trans-generational effect of CeO<sub>2</sub> NPs and found  
28 that second generation seedlings grown with seeds from treated parental plants with 10  
29 mg/L CeO<sub>2</sub> NPs were significantly smaller and accumulated more cerium as compared to  
30 seedlings generated from control plants (11). Ma et al. (12) studied how rare earth oxide  
31 NPs affected root elongation and found that bare CeO<sub>2</sub> NPs with an average diameter of  
32  $7.2 \pm 0.7$  nm had no effects on rape (*Brassica napus* L.), radish (*Raphanus sativus* L.),  
33 wheat (*Triticum aestivum* L.), cabbage (*Brassica oleracea* L.), tomato (*Lycopersicon*  
34 *esculentum* L.), and cucumber (*Cucumis sativus* L.) at 2,000 mg/L. Rico et al. (13)  
35 demonstrated that exposing rice seedlings to bare CeO<sub>2</sub> NPs with an average size of  $231$   
36  $\pm 16$  nm up to 500 mg/L for ten days caused no visible signs of toxicity. However, CeO<sub>2</sub>  
37 NPs induced a concentration-dependent modification of the oxidative stress and  
38 antioxidant defense system in the rice seedlings. Several studies have reported the uptake  
39 and accumulation of CeO<sub>2</sub> NPs by agricultural crops. For instance, Zhang and colleagues  
40 (14) showed that 7 nm and 25 nm bare CeO<sub>2</sub> NPs were detected in cucumber tissues but  
41 the transport of cerium from roots to shoots was limited. Zhao et al. (15) investigated the  
42 effects of bare and alginate coated CeO<sub>2</sub> NPs on corn plants and reported that surface  
43 coating and soil organic matter could promote the translocation of cerium in higher plants.  
44 A recent study demonstrated that intact CeO<sub>2</sub> NPs (7 nm) were taken up by soybean roots  
45 (16). In summary, CeO<sub>2</sub> NPs can be taken up by plants and accumulated in plant tissues,  
46 but the majority of the NPs appeared to remain in the root tissues, raising concerns on the  
47 heightened accumulation of ENMs by root vegetables.

48            Interestingly, even though the edible tissues of belowground vegetables often  
49 have direct contact with soil-borne ENMs and present the highest potential for ENMs  
50 accumulation in food crops, little attention has been paid to this important group of food  
51 plants. In this study, radish (*Raphanus sativus* L.) was adopted as a model plant in that it  
52 is a popular vegetable with high global consumption. In addition, radishes mature rapidly  
53 in full sun and light, and can be harvested in 3-4 weeks, making it an ideal plant to study  
54 the fate and impact of environmental chemicals on the development of belowground  
55 vegetables. The objectives of this study were two-fold: 1) how does cerium in different  
56 chemical forms (e.g. ionic cerium vs. cerium particles) and physical sizes affect the  
57 growth of radish? (2) How extensively and differently will the radish tissues take up and  
58 accumulate cerium in different forms and sizes? With these two objectives, we aimed to  
59 fill some of the current knowledge gap on the possible differential accumulation of  
60 cerium with different forms and particles sizes by plants. Even though detailed studies on  
61 the cerium effect of essential physiological and biochemical processes are not the  
62 concentration of this study, their interactions are important for mechanistic understanding  
63 of the interactions of plants and nanoparticles and warrant further investigations.

64

## 65 **Materials and Methods**

66

### 67 **Chemicals**

68            Dispersions of CeO<sub>2</sub> NPs (10 wt. % in H<sub>2</sub>O) and cerium chloride powder were  
69 purchased from Sigma-Aldrich (St. Louis, MO). The bulk powder of CeO<sub>2</sub> was obtained  
70 from Strem Chemicals, Inc. (Newburyport, MA). Hoagland solution (one-quarter  
71 strength) was prepared by dissolving an appropriate amount of the modified Hoagland  
72 basal salt mixture (Phytotechnology Laboratories, Lenexa, KS) with deionized water. The

73 size and morphology of CeO<sub>2</sub> NPs and the bulk suspensions were characterized by  
74 transmission electron microscopy (TEM). The hydrodynamic size and zeta potential of  
75 CeO<sub>2</sub> NPs in quarter strength Hoagland solution were measured with a dynamic light  
76 scattering instrument (Malvern Zetasizer Nano-ZS90, NY).

### 77 **Seed germination and growth conditions**

78 The radish seeds [Cherriette (F1)] were obtained from Johnny's Selected Seeds  
79 (Winslow, ME). Seeds were surface sterilized with 1.25% sodium hypochlorite solution  
80 for 10 minutes and then rinsed with deionized water three times. The sterilized seeds  
81 were germinated on moist filter paper in a Petri dish for 7 days. Healthy young seedlings  
82 with similar size (7.5 -8 cm in height from the root tip to the tip of cotyledons) and stage  
83 of development were transferred to 50 mL polypropylene centrifuge tubes containing  
84 quarter strength Hoagland solution and were incubated in a growth cart with a 16 hrs-  
85 light/8 hrs-dark cycle (28 °C) to allow the seedlings to further develop. The growth cart  
86 was equipped with four T5 fluorescent tubes, providing a light intensity of approximately  
87 104  $\mu\text{mol m}^{-2}\cdot\text{s}^{-1}$  of visible light (400 ~ 700 nm) at the height of plant leaves. After 7  
88 days, the seedlings were transferred from the centrifuge tubes to 100 mL glass jars  
89 containing 10 mg/L of bulk or nano-sized cerium oxide (CeO<sub>2</sub>) or cerium chloride  
90 (CeCl<sub>3</sub>). Each jar had a floating lid made by Hareline 2 mm thin fly foam (Fishwest,  
91 Sandy, UT) so that the plant roots were constantly submerged in the treatment solutions.  
92 Due to the scarcity of information on the potential adsorption of cerium on foam surface,  
93 it was assumed that the potential impact of foam on cerium bioavailability was  
94 insignificant in this study. Four treatments were prepared, all in quarter strength  
95 Hoagland solution: (1) control (no cerium treatment), (2) 10 mg/L CeO<sub>2</sub> NPs, (3) 10



96 mg/L CeO<sub>2</sub> bulk, and (4) 10 mg/L CeCl<sub>3</sub>. The concentration of 10 mg/L was chosen  
97 because this value is considered environmentally relevant (18) and our previous studies  
98 also showed that CeO<sub>2</sub> NPs at this concentration slightly enhanced plant growth (10,11).  
99 Each treatment had 12 replicates. The solutions in the jars were replenished every other  
100 day with the same treatment solution to compensate for evapotranspiration, with the  
101 assumption that Ce would be taken up concurrently with water by plants. However, if  
102 plants preferably take up water, it is possible that cerium would accumulate in the  
103 growing solution. Plants were harvested 35 days after germination (i.e., 21 days after  
104 treatment). Additionally, a separate set of radish plants were grown and treated exactly as  
105 above. The harvested tissues from these plants were used to determine the distribution of  
106 cerium across the fine root tips and storage roots microscopically (see below for details).

### 107 **Plant physiological responses**

108 For the first batch of plants, daily transpiration rate was recorded for each  
109 seedling after they were transferred to 100 mL glass jars by measuring the water surface  
110 drop before the solution replenishment. The cumulative transpiration of each treatment  
111 was then calculated by summing the daily transpiration over the 21 d treatment period.  
112 Relative chlorophyll content was measured with a SPAD 502 Plus Chlorophyll Meter  
113 (Spectrum Technologies, Inc. Aurora, IL) one day prior to harvest and was expressed as a  
114 percent of control. An OS1p chlorophyll fluorometer (Opti-sciences, Inc. Hudson, NH)  
115 was used to measure the yield of quantum efficiency of PSII (light-adapted Y(II)) and the  
116 photochemical efficiency of PSII (dark-adapted F<sub>v</sub>/F<sub>M</sub>) on the same day the relative  
117 chlorophyll was measured. Five of the 12 replicates from each treatment were used in a  
118 leakage test to assess root membrane integrity. The leakage test followed the published

119 procedures with some modifications (19). Briefly, the entire fine root system was  
120 submerged in 50 mL of deionized water and the initial conductivity  $C_w$  was measured  
121 immediately (Orion ROSS Ultra pH/ATC Triode Orion Star A325 Thermo Fisher  
122 Scientific, Waltham, MA). The conductivity of the solution was measured again as  $C_0$   
123 after 3 hours of incubation at room temperature. The entire fine roots were then  
124 autoclaved at 121°C for 20 min with a Tuttnauer Brinkman 3850M autoclave to release  
125 all electrolytes. The final conductivity  $C_t$  was measured after the samples cooled to room  
126 temperature. The percentage of electrolyte leakage was calculated as:  $EL = (C_0 - C_w) / (C_t -$   
127  $C_w) \times 100$ .

#### 128 **Uptake, accumulation and distribution of cerium**

129 At harvest, radish plants were separated into fine roots, storage roots (the edible  
130 radish bulb), and shoots. The tissues were then dried in an oven at 75 °C for 7 days and  
131 their dry weights determined. For each treatment, the 12 storage roots and 12 shoot  
132 tissues were divided into to four groups respectively. The shoot and storage root tissues  
133 in each group were then ground together into fine powders, from which 0.25 g of the  
134 ground tissues were weighed and digested in 4 mL of 70% nitric acid and swirled to mix.  
135 For the fine roots, the remaining seven replicates (five replicates used for the electrolyte  
136 leakage test were excluded) were divided into three groups and each group contained  
137 either two or three of the fine root systems. Due to the smaller biomass of the fine roots,  
138 all ground tissues from each group were used for the digestion. The nitric acid digest was  
139 heated at 95 °C for 20 minutes and then 45 °C for 4 minutes, and the cycle was repeated  
140 5 times until all the dry tissues were dissolved. Afterwards, 2 mL of hydrogen peroxide  
141 was added to the mixture and heated using the same temperature cycle until the solution

142 was clear. The digest solution was then analyzed by inductively coupled plasma – mass  
143 spectrometry (ICP-MS) to obtain the concentration of cerium in each sample.

144         The radish roots used to determine the localization and distribution of cerium in  
145 their fine roots and storage roots were harvested at day 21 after treatment. To obtain a  
146 reference for the anatomy of the radish storage root, a cross section of the radish storage  
147 root taken at the equator was cut with a razor blade and observed under a Kruss  
148 MBL3000 light microscope (A.KRÜSS Optronic, Hamburg, Germany) (Supplementary  
149 Figure 1). The radish fine root tips and sections of the storage roots from each treatment  
150 were also examined using a Zeiss LSM 510 META confocal microscope. A laser  
151 excitation wavelength of 543 nm was used and an emission filter band pass was set  
152 between 530-590 nm to collect both the laser reflection and autofluorescence in this  
153 region. To image the storage root, the root was first cut in half horizontally from the  
154 thickest point and then a thin slice (~ 1mm) of the storage root was cut from the bottom  
155 half of the storage root. That slice was then divided into four quarters and one of the  
156 quarters was randomly selected to determine the radial distribution of cerium toward the  
157 midpoint of the storage root. A schematic illustration of the slices preparation is shown in  
158 Supplementary Figure 1. For each sample, a serial scanning along the z-axis of the  
159 sample was conducted and the numbers of scanning planes varied from 8 to 11. The  
160 distance between two optical planes was approximately 10.2  $\mu\text{m}$ .

#### 161 **Data Analysis**

162         A one-way ANOVA was performed in this study for data analysis. The Duncan  
163 test was conducted for post hoc comparisons.

164

165 **Results**

166 **Characterization of CeO<sub>2</sub> NPs and the bulk**

167           Supplementary Figure 2 shows the TEM images of CeO<sub>2</sub> NPs and bulk CeO<sub>2</sub> in  
168 quarter strength Hoagland solution. The nanoparticles displayed variable shapes and  
169 sizes. Individual nanoparticles possessed triangular, rectangular and other irregular  
170 shapes. The images indicate that the average diameter of individual CeO<sub>2</sub> NPs ranged  
171 from 10 – 30 nm. The nanoparticles aggregated considerably in the Hoagland solution,  
172 due to the high ionic strength. The hydrodynamic diameter of the nanoparticle aggregates  
173 was ~600 nm as measured by the DLS. The zeta potential of CeO<sub>2</sub> NPs in the Hoagland  
174 solution was approximately -11.9 mV, suggesting that the nanoparticles were not stable.  
175 Bulk CeO<sub>2</sub> were mostly at the micron scale but the sizes were not uniform. Particles at  
176 the nanoscale were also detected in the bulk solutions. The sizes of bulk CeO<sub>2</sub> ranged  
177 approximately from 100 nm to 4,000 nm.

178 **Plant physiological status**

179           The radish exposed to CeO<sub>2</sub> bulk had the highest total dry biomass and was  
180 significantly greater than all other treatments (Figure 1a). The biomass of the  
181 nanoparticle treated plants was not significantly different from the control plants. The  
182 plant biomass exposed to cerium ions was significantly lower than all other treatments.  
183 When the plant tissues were examined separately, the bulk cerium treated radishes, which  
184 had similar shoot biomasses as CeO<sub>2</sub> NPs-treated radishes, had significantly higher dry  
185 shoot biomass than control and cerium ions treatment (Figure 1b). The dry weight of  
186 storage roots across the treatments exhibited similar patterns as the total dry biomass  
187 (Figure 1c), but the dry biomass of fine roots did not differ significantly as a function of

188 treatment (Figure 1d). In addition to the total biomass, the distribution of the biomass  
189 between the root (fine + storage root) and shoot compartments was significantly different  
190 in response to treatment. The shoot/root ratio of dry biomass of cerium ion treated radish  
191 ( $1.34 \pm 0.11$ ) was significantly higher ( $p < 0.05$ ) than all other treatments, which had  
192 similar ratios (control:  $1.00 \pm 0.10$ ; bulk CeO<sub>2</sub>:  $0.95 \pm 0.06$ ; CeO<sub>2</sub> NPs:  $1.07 \pm 0.07$ ).  
193 Visually, there was no apparent adverse effect of any of the cerium treatments on growth  
194 and development of the radish plants except for the size differences (Figure 1e).

195 In addition to the root biomass, the fine root membrane integrity was significantly  
196 affected by different forms of cerium. Figure 2 indicates that 10 mg/L of CeO<sub>2</sub> NPs and  
197 ionic cerium resulted in significantly greater electrolyte leakage when compared to the  
198 control roots. Leakage from bulk cerium treated roots was not significantly different from  
199 control roots. The accumulative transpiration of radish for all treatments was comparable  
200 until day 21, since then the accumulative transpiration of cerium ion treated radish  
201 became significantly lower than other treatment groups (Supplementary Figure 3). The  
202 relative chlorophyll content expressed in percentage is shown in Table 1. Although all  
203 treated radishes had lower chlorophyll content, only the bulk CeO<sub>2</sub> and CeO<sub>2</sub> NPs treated  
204 leaves had significantly lower chlorophyll content compared to the controls. The average  
205 quantum yield of photosystem II (Y(II)) and the  $F_v/F_m$  ratio for plants from different  
206 treatments are also shown in Table 1. The results indicated that the Y(II) was unaffected  
207 by the treatments. In contrast, only bulk CeO<sub>2</sub> treated radishes displayed an  $F_v/F_m$  ratio  
208 significantly lower value than the control. No significant differences were observed  
209 between the other cerium treatments.

## 210 **Cerium uptake and accumulation**

211 Not surprisingly, exposure to cerium resulted in significantly greater  
212 concentrations of this element in plant tissues. For the treated plants, the cerium  
213 concentration and content were significantly higher in the fine roots than in other tissues  
214 (Figure 3a-d). Among different treatments, the concentration of cerium in the storage root  
215 was not significantly different between cerium treatments (Figure 3a). In the shoot  
216 tissues, cerium ion treated radish had highest cerium concentration, followed by bulk  
217 cerium and then CeO<sub>2</sub> NPs treated radish (Figure 3a). The fine roots of CeO<sub>2</sub> NPs treated  
218 radish had significantly higher concentration of cerium than the bulk and ion treated  
219 radish (Figure 3b). When the cerium content rather than the concentration in different  
220 tissues was compared, cerium content in the storage roots of different treatments was still  
221 similar. The shoot cerium content of bulk and ion treated radishes was not significantly  
222 different but was markedly higher than nanoparticle treated radishes (Figure 3c). In the  
223 fine roots, the cerium content demonstrated similar patterns as the cerium concentration  
224 for different treatments (Figure 3d).

#### 225 **Cerium localization and distribution in radish root and storage root**

226 For the fine root tips, the confocal microscopic images were captured both on the  
227 surface and at different depths from the surface. The control had some weak signals from  
228 either the cerium content in control tissues or from background excitation (Figure 4a). In  
229 contrast, plant roots from treated plants all generated stronger signals (Figure 4b-f).  
230 However, the signal patterns were noticeably different. On the bulk CeO<sub>2</sub> treated root, the  
231 signals were only detected from the mucilage surrounding the root tip in both surface and  
232 deeper scanning images (Figure 4b,c). CeO<sub>2</sub> NPs were detected on larger areas of the root  
233 surface as well as the mucilage on the root tip of the nanoparticle treated plants (Figure

234 4d). The signal was even more prominent in the deeper scanning planes (Figure 4e). For  
235 cerium ion treated radish root, the signals were predominantly detected in the  
236 surrounding areas. Neither the surface scan nor the deep scan detected significantly  
237 stronger signals than the controls within the root itself (Figure 4f).

238 Figure 5 shows the confocal images of cut slices of radish storage roots. The  
239 control storage root showed little signal (Figure 5a). In comparison, storage roots from  
240 treated plants had strong signals. For bulk CeO<sub>2</sub> treated radish, all signals came from the  
241 pigmented periderm with a random pattern (Figure 5b). For CeO<sub>2</sub> NPs treated radish,  
242 stronger signals were observed in the pigmented periderm. In addition, the nanoparticles  
243 appeared to penetrate further into the storage root (Figure 5c). Cerium was not only  
244 detected in the periderm but also in the secondary vascular tissues in the storage root of  
245 cerium ion treated radish (Figure 5d,e).

246

## 247 **Discussion**

248 Accompanied with the ever expanding applications of engineered nanomaterials  
249 are the increasing concerns about their toxicity to humans and the environment. A major  
250 question scientists are trying to ascertain is whether the reduction of micro-sized particles  
251 to nano-sized particles will significantly increase their toxicity. Several previous studies  
252 have shown that nanoparticles typically exhibit stronger effect on plants than their bulk  
253 counterparts (20, 21). For example, following a 15-day hydroponic exposure, the biomass  
254 of zucchini plant exposed to silver nanoparticles was 75% less than plants treated with  
255 same concentrations of bulk silver powder (21). For CeO<sub>2</sub> particles, it is well accepted  
256 that the presence of highly mobile lattice oxygen on the surface will cause oxygen

257 vacancy on the surface (22). With the decrease of nanoparticle size, the specific surface  
258 area and consequently the density of the oxygen vacancy increase. The separation of  
259 oxygen from the lattice structure generates electrons which can be used to reduce  $Ce^{4+}$  to  
260  $Ce^{3+}$ . With increasing oxygen vacancy, the ratio of  $Ce^{3+}/Ce^{4+}$  will increase on the surface  
261 of nanoparticles (23). Because  $Ce^{3+}$  is about 14% larger than  $Ce^{4+}$  (22), the conversion of  
262  $Ce^{4+}$  to  $Ce^{3+}$  will strain the lattice structure and increase the reactivity and the superoxide  
263 dismutase (SOD) mimetic activity of the  $CeO_2$  particles (24). Therefore, particle size is  
264 an important consideration in the assessment of the environmental toxicity of  $CeO_2$ .  
265 Unfortunately, information on the size effect of  $CeO_2$  particles on plant development in  
266 the literature is very limited.

267         Due to the potential dissolution of some metallic nanoparticles, another major  
268 question actively investigated in the scientific community of nanotoxicology is the  
269 comparative toxicity of nanoparticles and the ionic form of the particles. Because of the  
270 general acceptance that  $CeO_2$  NPs are stable in liquid solutions, ionic cerium was  
271 generally not included in the treatment paradigms (13-16). However, the broad  
272 applications of different forms and sizes of cerium require a comprehensive  
273 understanding and comparison of their fate and phytotoxicity. Our investigation provides  
274 an assessment of the differential fate and phytotoxicity of cerium in its ionic, nanoscale  
275 and bulk particle forms. Several physiological parameters including the root membrane  
276 integrity photosynthesis-related measurements, and biomass parameters were affected by  
277 certain forms of cerium at the tested concentration.

278         While the specific mechanisms by which cerium compounds may compromise  
279 membrane integrity are not known and may differ, all forms and sizes of cerium resulted



280 in some damage to root membrane integrity as indicated by an increase in electrolyte  
281 leakage. The effect was significant however only for the nanoparticle and ionic forms.  
282 The changes in the integrity of root membrane could also alter the membrane potential  
283 and potentially the function of the membrane (24). It has been reported that altered  
284 plasma membrane integrity and potential is associated with changes in the ion fluxes into  
285 plant roots (25). Whether this alteration of membrane integrity influenced the  
286 concentration of any essential macronutrients or micronutrients in radish was not  
287 examined but would be a reasonable question for future studies. For the bulk CeO<sub>2</sub> and  
288 CeO<sub>2</sub> NPs, in addition to their impact on the membrane, physical adsorption on root  
289 surface and blockage of nutrient uptake by plant roots may also occur. It is possible that  
290 such impacts on the roots may have affected the uptake of elements such as magnesium  
291 or iron, two nutrients associated with the synthesis of chlorophyll. A decrease in the  
292 concentration of either of these essential nutrients might have contributed to the decrease  
293 in relative chlorophyll content observed in some treatments. Other aspects of chlorophyll  
294 synthesis or degradation could have been affected as well and a more detailed study will  
295 be required to understand the extent or severity of effects of cerium on chlorophyll  
296 metabolism. The significantly lower F<sub>v</sub>/F<sub>M</sub> values observed for the bulk cerium treatment  
297 as compared to the control plants suggested that photosynthetic electron transport  
298 associated with photosystem II was stressed in those plants, but not for the other cerium  
299 treatments. These results differ from a study with plantlets of *Medicago arborea* in  
300 which nanoceria was found to have a more negative effect on the F<sub>v</sub>/F<sub>M</sub> ratio than the  
301 same concentrations of bulk cerium (25). Other studies have shown that the influence of  
302 cerium compounds on plant photochemistry differs depending on factors such as plant

303 Mn status (26,) and the presence of salt stress (27). Definitive conclusions about the  
304 comparative phytotoxicity of the cerium ion and nanoceria cannot be made without  
305 further investigation. Even so, the overall effect of all treatments on the two  
306 photosynthetic parameters measured were modest and perhaps not indicative of a  
307 significant stress imposed on the plants, particularly given that there were no overt visible  
308 effects observed for any treatments, including the ionic cerium and the CeO<sub>2</sub> NPs  
309 treatments. The only other indication of a negative effect of treatment with cerium was  
310 the decrease in biomass observed for the cerium ion treatment.

311         The shoot/root ratio of radish was also affected by cerium, primarily through the  
312 change of the biomass of the storage roots. Because the root thickening is a result of the  
313 combined cell division and enlargement of secondary xylem and phloem cells which  
314 depends on the activity of the vascular cambium (28), it is possible that the cerium of  
315 different forms have different impacts on the activity of the vascular cambium. One could  
316 speculate that the bulk CeO<sub>2</sub> might have enhanced the activity of the vascular cambium  
317 while ionic Ce inhibited it. Metabolically, according to the “sink capacity” theory, the  
318 storage root represents a major reservoir for radish and sucrose transported within radish  
319 is the main carbohydrate for the growth of sinks. As such, photosynthate distribution into  
320 different tissues is heavily affected by the activity of sucrose synthase (SuSy) (29-32). If  
321 future studies examined the expression of SuSy genes and/or measured the activity of this  
322 enzyme in the radish hypocotyl in response to different forms of cerium, it might be  
323 possible to ascertain whether the changes in the mass of the storage root in response to  
324 bulk or ionic cerium treated radish plants were due to changes in sink strength. The  
325 specific mechanisms by which these cerium compounds influence the biomass of radish

326 storage roots has implications for the agricultural production of radish and related  
327 vegetable species and are therefore worth further attention.

328           It should be pointed out that concentration of  $\text{CeCl}_3$  used in this study was very  
329 low and the impact of chloride ion is not expected to be substantial. Parida and Das (33)  
330 investigated plant salt tolerance and salinity effects on plant growth and the authors  
331 reported that under 100 mM NaCl (3.55 g/L  $\text{Cl}^-$ ), chloride demonstrated limited influence  
332 on the osmotic adjustment of cell membrane. Scialabba and Melati (34) also reported that  
333 sodium chloride up to a concentration of 0.1% positively affected radish growth. The  $\text{Cl}^-$   
334 in the ionic cerium solution used in this study was significantly lower than those reported  
335 values and was not expected to significantly contribute to the negative effect observed in  
336 the ionic treatment group. Consequently, the negative effect observed in the ionic  
337 treatment should be attributed to the ionic cerium. Another caveat about the results is that  
338 10 mg/L was the concentration of the compounds of  $\text{CeO}_2$  and  $\text{CeCl}_3$ , not the  
339 concentration of cerium as an element. Due to the different molecular weight percentage  
340 of cerium in  $\text{CeO}_2$  and  $\text{CeCl}_3$ , the actual concentration of cerium as an element was 8.14  
341 mg Ce/L in  $\text{CeO}_2$  NPs and the bulk and was only 5.68 mg Ce/L in the ionic form. Cerium  
342 in  $\text{CeO}_2$  was 43.5% higher than in the ionic form. If the equivalent concentration of  
343 cerium as an element was used, the ionic cerium may display an even stronger effect on  
344 plant physiology.

345           In addition to the yield of edible storage root, the potential accumulation of  
346 cerium was examined. Exposed plants had detectable cerium in all plant tissues,  
347 including the edible storage roots and leaves even though the forms of cerium in these  
348 tissues are unknown. However, the forms of cerium in plant tissues may affect both their

349 toxicity and potential availability to humans and they deserve detailed investigation in  
350 future studies. In current study, the significantly higher cerium detected in the shoot  
351 tissues of exposed plants indicated that cerium translocation from roots to shoot had  
352 occurred. The upward transport of bulk cerium to radish shoots was unexpected given the  
353 size of the particles and the low dissolution rate of bulk CeO<sub>2</sub>. It is most likely that the  
354 cerium content detected from the bulk treated shoot tissues was from the nanoscale  
355 particles present in the bulk mixture (Supplementary Figure 2). The upward transport of  
356 CeO<sub>2</sub> NPs and ionic cerium from roots to shoots was expected and has been reported in  
357 the literature (10, 14, 35). Interestingly, however, when the cerium localization in the  
358 storage root was investigated with the confocal microscope, signals of cerium in the  
359 vascular tissues were only observed in cerium ion treatment, suggesting that active  
360 transport may function as an important pathway of cerium accumulation only for ion  
361 treated radishes. In contrast, signals from the CeO<sub>2</sub> NPs and bulk treated radish roots  
362 were mainly located on the periderms. The results suggest that adsorption and diffusion  
363 of particulate cerium along the radial direction might be a more important pathway for  
364 CeO<sub>2</sub> NPs and bulk accumulation in radish storage roots. The diffusion may possibly  
365 occur from the lenticels on the periderm, but more precise techniques are needed to  
366 confirm this assumption. From the food safety point of view, the cerium accumulation in  
367 the edible storage root is more concerning and our results showed that while cerium  
368 concentration and content were similar across the cerium treatment, the distribution of  
369 cerium in the storage roots varied and consequently their availability to humans would  
370 vary. For example, the majority of particulate cerium accumulated in the edible tissue  
371 could be removed in the food preparation process while ionic cerium in the storage roots

372 is more likely to be consumed by humans with the storage root.

373 In closing, our results suggested that 10 mg/L cerium as cerium oxide or cerium  
374 chloride could affect the growth of radish and could accumulate in the edible storage root  
375 and shoot tissues. However, the impact and accumulation patterns varied significantly by  
376 the size and chemical form of cerium. Ionic cerium displayed the strongest impact on  
377 radish root membrane integrity and growth, followed by CeO<sub>2</sub> NPs and then the bulk.  
378 While cerium of different forms all accumulate in radish tissues, their accumulation  
379 potential and distribution patterns varied greatly. As a result, potential exposure and risk  
380 to human health through diet exposure to different sizes and forms of cerium may vary  
381 and these differences should be considered when evaluating the food safety of cerium in  
382 the environment.

383

#### 384 **Acknowledgement**

385 The authors acknowledge the financial support of the USDA-AFRI (#2012-67005-19585)  
386 and USDA-AFRI (#2011-67006-30181).

387

#### 388 **Supporting Information Available**

389 The transmission electron microscopic images of bulk CeO<sub>2</sub> and CeO<sub>2</sub> NPs, the  
390 accumulative transpiration of radish plants and the anatomy of radish storage root were  
391 provided as supporting information. This information is available free of charge via the  
392 Internet at <http://pubs.acs.org>.

393

394

395 **References**

- 396 (1) Tiede, K.; Hassellöv, M.; Breitbarth, E.; Chaudhry, Q.; Boxall, A., Considerations for  
397 Environmental Fate and Ecotoxicity Testing to Support Environmental Risk  
398 Assessments for Engineered Nanoparticles. *J. Chromatogr. A.* **2009**, *1216*(3), 503-  
399 509.
- 400 (2) Nowack, B.; Bucheli, T. D., Occurrence, Behavior and Effects of Nanoparticles in the  
401 Environment. *Environ. Pollut.* **2007**, *150*(1), 5-22.
- 402 (3) Bystrzejewska-Piotrowska, G.; Golimowski, J.; Urban, P. L., Nanoparticles: Their  
403 Potential Toxicity, Waste and Environmental Management. *Waste Manage.* **2009**,  
404 *29*(9), 2587-2595.
- 405 (4) Brar, K.; Verma, M.; Tyagi, R. D.; Surampalli, R. Y. Engineered Nanoparticles in  
406 Wastewater and Wastewater Sludge – Evidence and Impacts. *Waste Manage.* **2010**,  
407 *30*(3), 504-520.
- 408 (5) Been, T. M.; Westerhoff, P. Nanoparticle Silver Released into Water from  
409 Commercially Available Sock Fabrics. *Environ. Sci. Technol.* **2008**, *42*(11), 4133–  
410 4139.
- 411 (6) Limbach, L. K.; Bereiter, R.; Müller, E.; Krebs, R.; Gälli, R.; Stark, W. J. Removal of  
412 Oxide Nanoparticles in a Model Wastewater Treatment Plant: Influence of  
413 Agglomeration and Surfactants on Clearing Efficiency. *Environ. Sci. Technol.* **2008**,  
414 *42*(15), 5828–5833.
- 415 (7) Pelletier, D. A.; Suresh, A. K.; Holton, G. A.; McKeown, C. K.; Wang, W.; Gu, B.;  
416 Mortensen, N. P.; Allison, D. P.; Joy, D. C.; Allison, M. R.; Brown, S. D.; Phelps, T.  
417 J.; Doktycz, M. J. Effects of Engineered Cerium Oxide Nanoparticles on Bacterial  
418 Growth and Viability. *Appl. Environ. Microbiol.* **2010**, *76*(24), 7981-7989.
- 419 (8) Rosenkranz, P.; Fernández-Cruz, M. L.; Conde, E.; Ramírez-Fernández, M. B.;  
420 Flores, J. C.; Fernández, M.; Navas, J. M. Effects of Cerium Oxide Nanoparticles to  
421 Fish and Mammalian Cell Lines: An Assessment of Cytotoxicity and Methodology.  
422 *Toxicol. in Vitro.* **2012**, *26*(6), 888-896.
- 423 (9) Zhu, H.; Han, J.; Xiao, J. Q.; Jin, Y. Uptake, Translocation, and Accumulation of  
424 Manufactured Iron Oxide Nanoparticles by Pumpkin Plants. *J. Environ. Monit.* **2008**,  
425 *10*(6), 713–717.
- 426 (10) Wang, Q.; Ma, X.; Zhang, W.; Pei, H.; Chen, Y. The Impact of Cerium Oxide  
427 Nanoparticles on Tomato (*Solanum Lycopersicum* L.) and Its Implications for Food  
428 Safety. *Metallomics.* **2012**, *4*(10), 1105-1112.
- 429 (11) Wang, Q.; Ebbs, S. D.; Chen, Y.; Ma, X. Trans-generational Impact of Cerium  
430 Oxide Nanoparticles on Tomato Plants. *Metallomics.* **2013**, *5*(6), 753-759.

- 431 (12) Ma, Y.; Kuang, L.; He, X.; Bai, W.; Ding, Y.; Zhang Z.; Zhao, Y.; Chai, Z. Effects  
432 of Rare Earth Oxide Nanoparticles on Root Elongation of Plants. *Chemosphere*. **2010**,  
433 78(3), 273–279.
- 434 (13) Rico, C. M.; Hong J.; Morales, M. I.; Zhao, L.; Barrios, A. C.; Zhang, J. Y.;  
435 Peralta-Videa, J. R.; Gardea-Torresdey, J. L. Effect of Cerium Oxide Nanoparticles on  
436 Rice: A Study Involving the Antioxidant Defense System and In Vivo Fluorescence  
437 Imaging. *Environ. Sci. Technol.* **2013**, 47(11), 5635-5642.
- 438 (14) Zhang, Z.; He, X.; Zhang, H.; Ma, Y.; Zhang, P.; Ding, Y.; Zhao, Y. Uptake and  
439 Distribution of Ceria Nanoparticles in Cucumber Plants. *Metallomics*. **2011**, 3(8),  
440 816-822.
- 441 (15) Zhao, L.; Peralta-Videa, J. R.; Varela-Ramirez, A.; Castillo-Michel, H.; Li, C.;  
442 Zhang, J.; Aguilera, R. J.; Keller, A. A.; Gardea-Torresdey, J. L. Effect of Surface  
443 Coating and Organic Matter on the Uptake of CeO<sub>2</sub> NPs by Corn Plants Grown in  
444 Soil: Insight Into the Uptake Mechanism. *J. Hazard Mater.* **2012**, 225, 131-138.
- 445 (16) Lopez-Moreno, M. L.; de la Rosa, G.; Hernandez-Viezcas, J.; Castillo-Michel, H.;  
446 Botez, C.; Peralta-Videa, J. R.; Gardea-Torresdey, J. L. Evidence of the Differential  
447 Biotransformation and Genotoxicity of ZnO and CeO<sub>2</sub> Nanoparticles on Soybean  
448 (*Glycine max*) Plants. *Environ. Sci. Technol.* **2010**, 44(19), 7315-7320.
- 449 (17) Boxall, A., Chaudhry, Q., Sinclair, C., Jones, A., Aitken, R., Jefferson, B., Watts,  
450 C. *Current and Future Predicted Environmental Exposure to Engineered*  
451 *Nanoparticles*. Central Science Laboratory, Department of the Environment and  
452 Rural Affairs, London, UK. **2007**.
- 453 (18) Sanchez-Viveros, G.; Gonzalez-Mendoza, D.; Alarcon, A.; Ferrera-Cerrato, R.  
454 Copper Effects on Photosynthetic Activity and Membrane Leakage of *Azolla*  
455 *Filiculoides* and *A. Caroliniana*. *Int. J. Agr. Biol.* **2010**, 12(3), 365-368.
- 456 (19) Feizi, H., Moghaddam, P. R., Shahtahmassebi, N., Fotovat, A. Impact of bulk and  
457 nanosized titanium dioxide (TiO<sub>2</sub>) on wheat seed germination and seedling growth.  
458 *Biol. Trace Elem. Res.* **2012**, 146(1), 101-106.
- 459 (20) Stampoulis, D., Sinha, S. K., White, J. C. Assay-dependent phytotoxicity of  
460 nanoparticles to plants. *Environ. Sci. Technol.* **2009**, 43(24), 9473-9479.
- 461 (21) Dutta, P., Pal, S., Seehra, M. S., Shi, Y., Eyring, M., Ernst, R. D. Concentration of  
462 Ce<sup>3+</sup> and oxygen vacancies in cerium oxide nanoparticles. *Chem. Mater.* **2006**, 18,  
463 5144-5146.
- 464 (22) Deshpande, S., Patil, S., Kuchibhatla, S. T., Seal, S. Size Dependency Variation in  
465 Lattice Parameter and Valency States in Nanocrystalline Cerium Oxide. *Appl. Phys.*  
466 *Lett.* **2005**, 87(13), 133113
- 467 (23) Heckert, E. G., Karakoti, A. S., Seal, S., Self, W. T. The Role of Cerium Oxide

- 468 State in the SOD Mimetic Activity of Nanoceria. *Biomaterials*. **2008**, 29(18), 2705-  
469 2709.
- 470 (24) Lindberg, S., Strid, H. Aluminium Induces Rapid Changes in Cytoplasmic pH and  
471 Free Calcium and Potassium Concentrations in Root Protoplast of Wheat (*Triticum*  
472 *aestivum*). *Physiol. Plantarum*. **1997**, 99(3), 405-414.
- 473 (25) Gomez-Garay, A., Pintos, B., Manzanera, J. A., Lobo, C., Villalobos, N., Martin,  
474 L. Uptake of CeO<sub>2</sub> Nanoparticles and Its Effect on Growth of *Medicago arborea* in  
475 Vitro Plantlets. *Biol. Trace. Elem. Res.*, **2014**, 161, 143-150,
- 476 (26) Qu, C., Liu, C., Guo, F., Hu, C., Ze, Y., Li, C., Zhou, Q., Hong, F. Improvement of  
477 Cerium on Photosynthesis of Maize Seedlings Under a Combination of Potassium  
478 Deficiency and Salt Stress. *Biol. Trace. Elem. Res.*, **2014**, 155, 104-113.
- 479 (27) Qu, C., Gong, X., Liu, C., Hong, M., Wang, L., Hong, F. Effects of Manganese  
480 Deficiency and Added Cerium on Photochemical Efficiency of Maize Chloroplasts.  
481 *Biol. Trace. Elem. Res.*, **2012**, 146, 94-100.
- 482 (28) Wherrett, T., Ryan, P. R., Delhaize, E., Shabala, S. Effect of Aluminum on  
483 Membrane Potential and Ion Fluxes at the Apices of Wheat Roots. *Funct. Plant Biol.*  
484 **2005**, 32(3), 199-208.
- 485 (29) Zaki, H. E. M., Takahata, Y., Yokoi, S. Analysis of the Morphological and  
486 Anatomical Characteristics of Roots in Three Radish (*Raphanus sativus*) Cultivars  
487 that Differ in Root Shape. *J. Hortic. Sci. Biotech.* **2012**, 87(2), 172-178.
- 488 (30) Farrar, J. F. Regulation of Shoot-root Ratio is Mediated by Sucrose. *Plant Soil.*  
489 **1996**, 185(1), 13-19.
- 490 (31) Rouhier, H.; Usuda, H. Spatial and Temporal Distribution of Sucrose Synthase in  
491 the Radish Hypocotyl in Relation to Thickening Growth. *Plant cell physiol.* **2001**,  
492 42(6), 583-593.
- 493 (32) Usuda, H.; Demura, T.; Shimogawara, K.; Fukuda, H. Development of Sink  
494 Capacity of the "Storage Root" in a Radish Cultivar with a High Ratio of "Storage  
495 Root" to Shoot. *Plant Cell Physiol.* **1999**, 40(4), 369-377.
- 496 (33) Wardlaw, I. F. The Control and Pattern of Movement of Carbohydrates in Plants.  
497 *Bot. Rev.* **1968**, 34(1), 79-105.
- 498 (34) Parida, A. K.; Das, A. B. Salt Tolerance and Salinity Effects on Plants: A Review.  
499 *Ecotox. Environ. Safe.* **2005**, 60(3), 324-349.
- 500 (35) Scialabba, A.; Melati, M. R. The Effect of NaCl on Growth and Xylem  
501 Differentiation of Radish Seedlings. *Bot. Gaz.* **1990**, 151(4), 516-521.
- 502 (36) Hu, X., Ding, Z., Chen, Y., Wang, X., Dai, L. Bioaccumulation of Lanthanum and

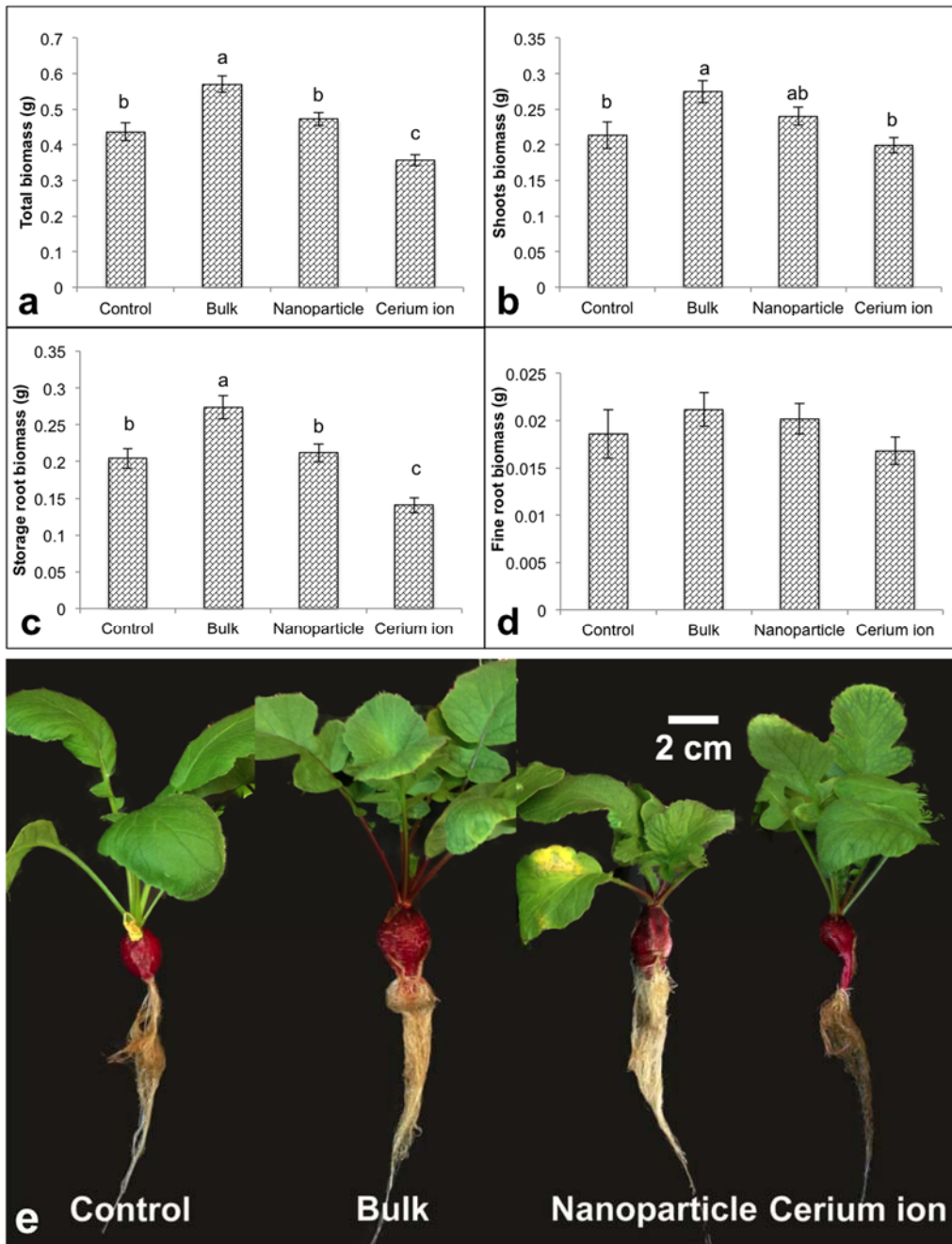


503 Cerium and Their Effects on the Growth of Wheat (*Triticum aestivum L.*) Seedlings.  
504 *Chemosphere*. **2002**, 48(6), 621-629.  
505  
506  
507  
508  
509  
510  
511  
512  
513  
514  
515  
516  
517  
518  
519  
520  
521  
522  
523  
524  
525  
526  
527  
528  
529  
530  
531  
532  
533  
534  
535  
536  
537  
538  
539  
540  
541  
542  
543  
544  
545  
546  
547

548 **Table 1:** The relative chlorophyll content expressed as percentage of control of each  
 549 treatment, the average Y(II), F<sub>v</sub>/F<sub>M</sub> ratio, n=12. Different letters in the table represent  
 550 significant differences between the treatments (p<0.05).  
 551

Treatment	Relative Chlorophyll (%)	Standard error	Y(II)	Standard error	F <sub>v</sub> /F <sub>M</sub>	Standard error
Control	100.00 <sup>a</sup>	2.67	0.774	0.007	0.830 <sup>a</sup>	0.003
Bulk	87.22 <sup>b</sup>	3.84	0.728	0.022	0.757 <sup>b</sup>	0.026
Nanoparticle	83.69 <sup>b</sup>	4.24	0.731	0.020	0.780 <sup>ab</sup>	0.016
Cerium ion	91.51 <sup>ab</sup>	4.68	0.697	0.060	0.797 <sup>ab</sup>	0.020

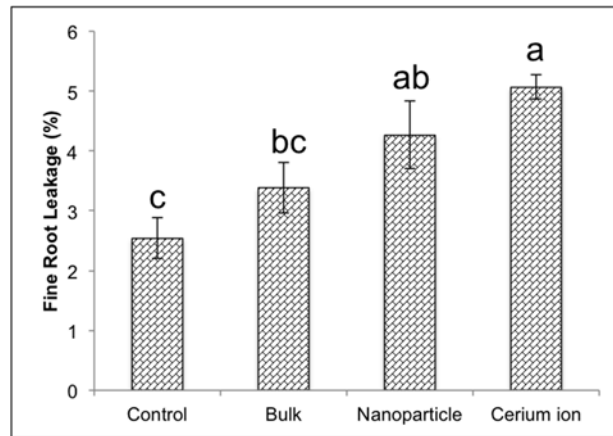
552  
 553  
 554  
 555  
 556  
 557  
 558  
 559  
 560  
 561  
 562  
 563  
 564  
 565  
 566  
 567  
 568  
 569  
 570  
 571  
 572  
 573  
 574  
 575  
 576  
 577  
 578  
 579  
 580  
 581  
 582  
 583  
 584  
 585  
 586  
 587



589  
 590  
 591  
 592  
 593  
 594  
 595  
 596  
 597  
 598  
 599

**Figure 1:** Dry biomass of total radish and different radish tissues treated with 10 mg/L of different forms of cerium (a-d). The reported values are the mean of 12 replicates and the error bars represent standard error. Different letters represent significant differences between the treatments ( $p < 0.05$ ). (e) Images of typical radish plants from the different treatments.

600



601

602

603 **Figure 2:** Electrolyte leakage from radish fine roots grown hydroponically in different

604 solutions. The reported values are the average of 5 replicates in each treatment and the

605 error bars represent standard error. Different letters represent significant differences

606 between the treatments ( $p < 0.05$ ).

607

608

609

610

611

612

613

614

615

616

617

618

619

620

621

622

623

624

625

626

627

628

629

630

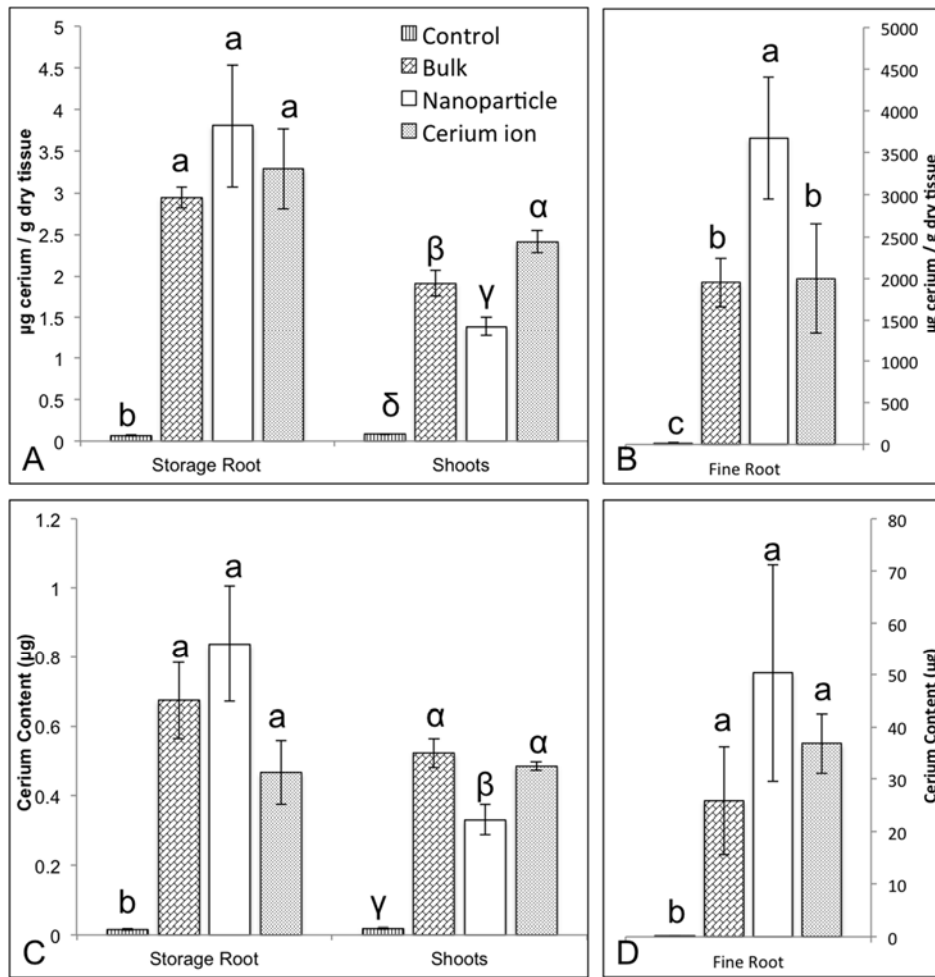
631

632

633

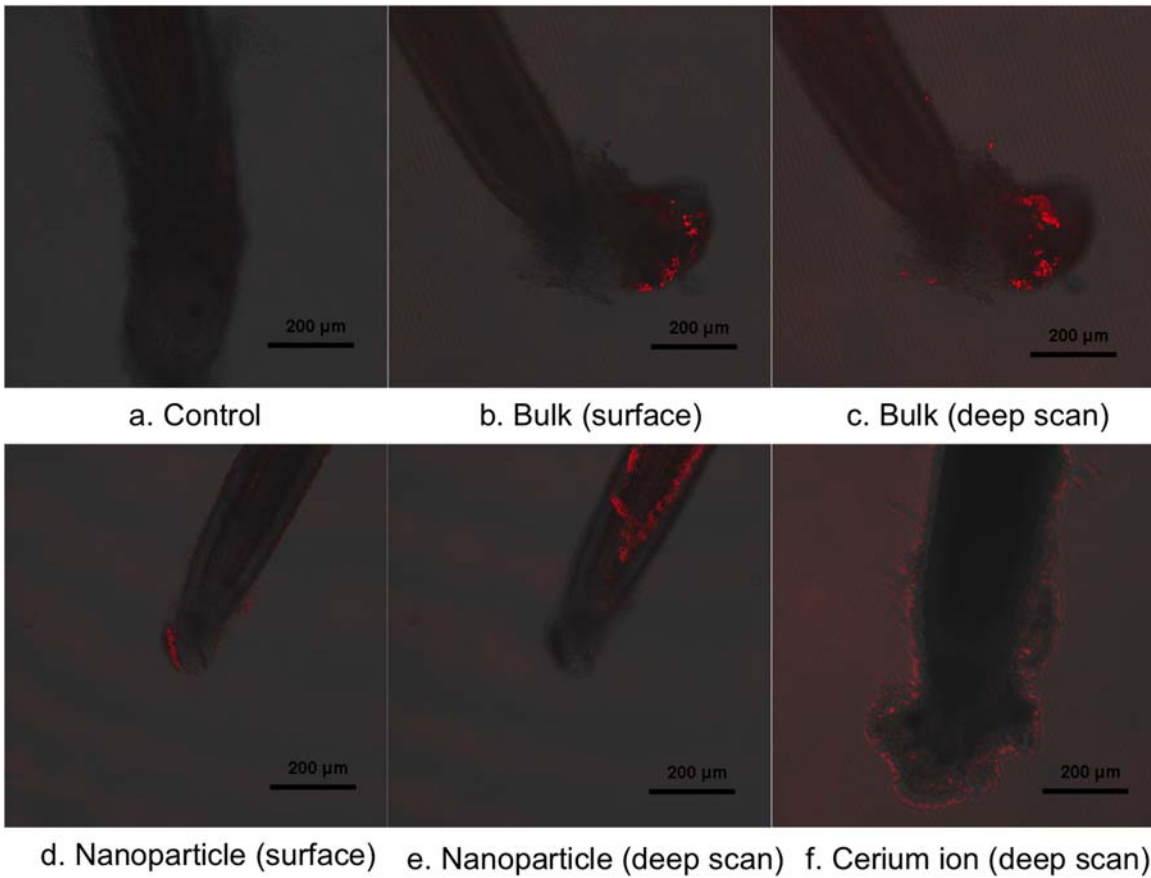
634

635



636  
637  
638  
639  
640  
641  
642  
643  
644  
645  
646  
647  
648  
649  
650

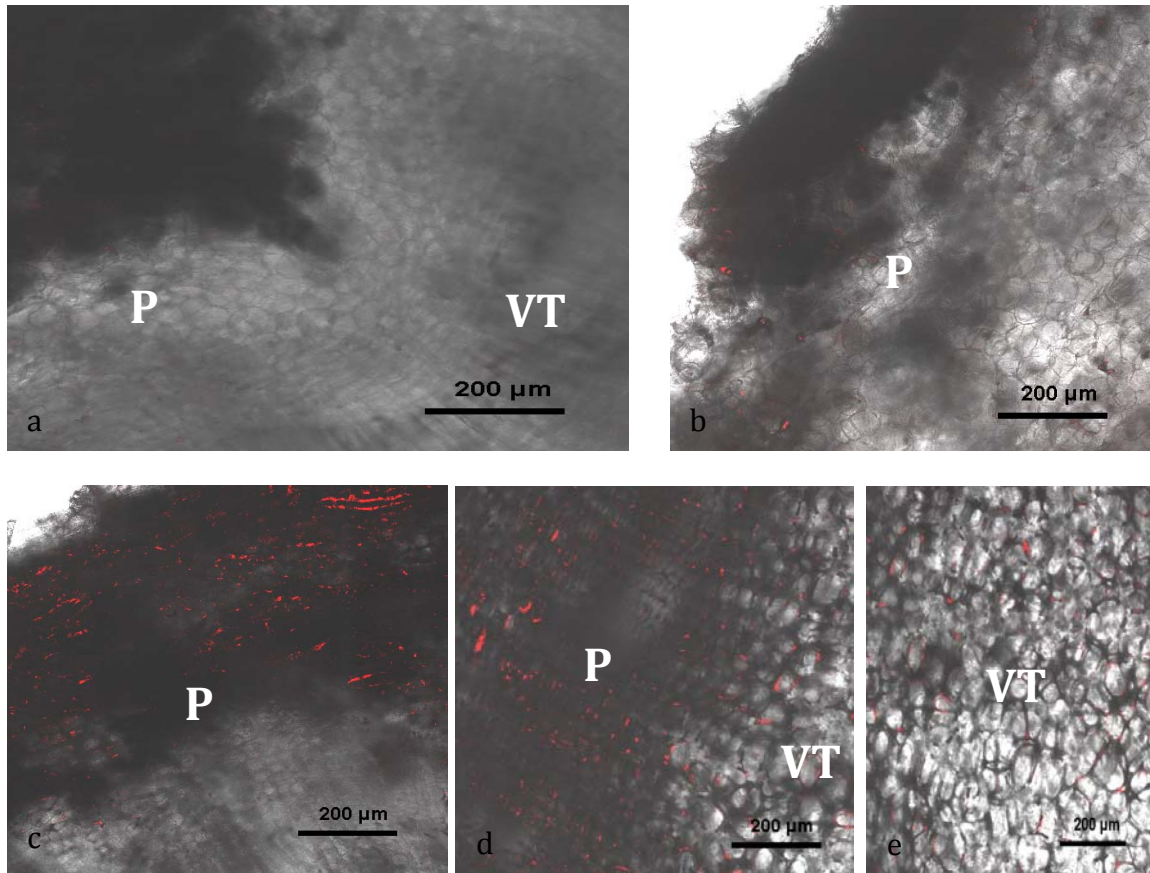
**Figure 3:** Cerium concentration (A and B) and mass (C and D) in different radish tissues. The reported values in A and C are the average of 4 measurements. The reported values in B and D are the average of 2 or 3 measurements. Errors bars represent standard error. Letters above bars reflect their statistical grouping. Different letters and Greek symbols represent significant differences between the treatments ( $p < 0.05$ ).



651  
 652  
 653  
 654  
 655  
 656  
 657  
 658  
 659  
 660  
 661  
 662  
 663  
 664  
 665  
 666  
 667  
 668  
 669  
 670  
 671  
 672  
 673  
 674

**Figure 4:** Confocal microscopic images depicting the accumulation of cerium in the fine roots of radish. (a) control root showing weak signals, (b, c) surface and representative deeper scan of fine roots treated by bulk CeO<sub>2</sub>, (d, e) surface and representative deeper scan of fine roots exposed to CeO<sub>2</sub> NPs and (f) a deeper scan image of fine roots exposed to cerium ion. The deeper scan images shown were selected from a stack of deep scan images for different roots.

675



676

677

678

679

680

681

682

683

684

685

686

687

688

689

690

691

692

693

694

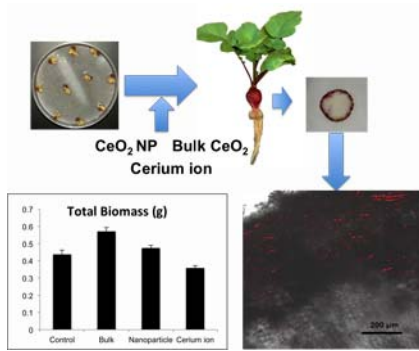
695

696

**Figure 5:** (a) Confocal images of the horizontal slices of radish storage root treated with different types of cerium. (a): control; (b): bulk CeO<sub>2</sub> treated radish; (c): CeO<sub>2</sub> NPs treated radish and (d, e): ionic cerium treated radish. P: Periderm; VT: Vascular tissues.

697  
698  
699

### TOC Graphic



700  
701  
702